



Cite this: *Chem. Sci.*, 2024, **15**, 10585

All publication charges for this article have been paid for by the Royal Society of Chemistry

Received 6th March 2024
Accepted 3rd June 2024

DOI: 10.1039/d4sc01569j
rsc.li/chemical-science

Introduction

In organic chemistry, the concept of isomers was initially introduced to describe the molecules that have the same molecular formula but different structural arrangements.^{1,2} Different isomeric structures induce their distinct properties and potential applications in the chemical and pharmaceutical industries.^{3–5} For instance, the isomeric (*R*)-thalidomide and (*S*)-thalidomide compounds exhibit different chemical properties, (*R*)-thalidomide is a sedative and (*S*)-thalidomide is a teratogen. Extending to nanoscale, since the first pair of nanocluster (NC) isomers were synthesized in 2015,⁶ several isomeric pairs have been reported, such as thiolated $\text{Au}_{38}(\text{SR})_{24}$,^{7,8 $\text{Au}_{36}(\text{SR})_{24}$,^{9,10 $\text{Au}_{28}(\text{SR})_{20}$,^{11,12} and $\text{Au}_{22}(\text{SR})_{15}$.¹³ With structural isomerization, their physical and chemical properties, including fluorescence,¹¹ catalysis,¹² thermal stability,¹⁴ and ultrafast electron dynamics⁹ have changed significantly. Compared with metal}}

nanoclusters, the exploration of the colloidal semiconductor magic-size cluster (MSC) isomers is still in its infancy. Until 2018, CdS MSC-311 and MSC-322 have been reported as the first pair of MSC isomers.^{15–17} Whereafter, only a few MSC isomers have been discovered.^{18–23} Overall, the reported NC isomers show available structure–property correlations, beneficial to their potential application as sensors, catalysts, etc.

However, the synthesis and discovery of NC isomers is generally unpredictable. Utilizing thermal stimuli is a common method for regulating the synthesis of NC isomers. For example, a pair of thermal responsive isomers, $\text{E-Au}_{13}\text{Ag}_{12}$ and $\text{S-Au}_{13}\text{Ag}_{12}$ NC were discovered¹⁴ by precise temperature control. This thermal stimulus effect is also effective in semiconductor MSCs.¹⁵ With applying the appropriate temperature stimuli, different structural MSC isomers were derived from an induction period sample. In this process, numerous trial experiments were conducted to establish the appropriate temperature range for obtaining various structural products. Another method for selective synthesis of NC isomers is ligand exchange.^{24–26} Typically, the stabilized NCs can transition to another stable state by introducing new ligands. Nonetheless, numerous works have been dedicated to seeking the appropriate ligands to ensure that the stabilized NCs can isomerize to another structure rather than transform into another species. In general, the reported synthetic strategies so far whether for metal or semiconductor NC isomers are empirical and lack prediction. A predictable and precise synthetic strategy, guided by clear principles, for selective synthesis of NC isomers with desired structure is immediately required. In organic synthesis, asymmetric catalysis serves as

^aCollege of Materials and Chemistry & Chemical Engineering, Chengdu University of Technology, Chengdu 610059, P. R. China. E-mail: zhangj0318@cdut.edu.cn; haoshi@cdut.edu.cn

^bKey Laboratory of Optoelectronic Devices and Systems of Ministry of Education and Guangdong Province, College of Physics and Optoelectronic Engineering, Shenzhen University, Shenzhen 518060, P. R. China. E-mail: songjun@szu.edu.cn

^cInstitute of Chemical Sciences and Engineering, Ecole Polytechnique Fédérale de Lausanne (EPFL), 1015 Lausanne, Switzerland

^dAntibiotics Research and Re-evaluation Key Laboratory of Sichuan Province, Sichuan Industrial Institute of Antibiotics, School of Pharmacy, Chengdu University, Chengdu 610106, P. R. China

† Electronic supplementary information (ESI) available. See DOI: <https://doi.org/10.1039/d4sc01569j>



a powerful tool for the selective synthesis of chiral molecules.^{27–29} During organocatalytic reactions, chiral small molecules are added by purpose as catalysts to decouple the structural parts of chiral products and obtain the desired ones. An open question is, can an analogous synthetic method be designed for selective synthesis of NC isomers?

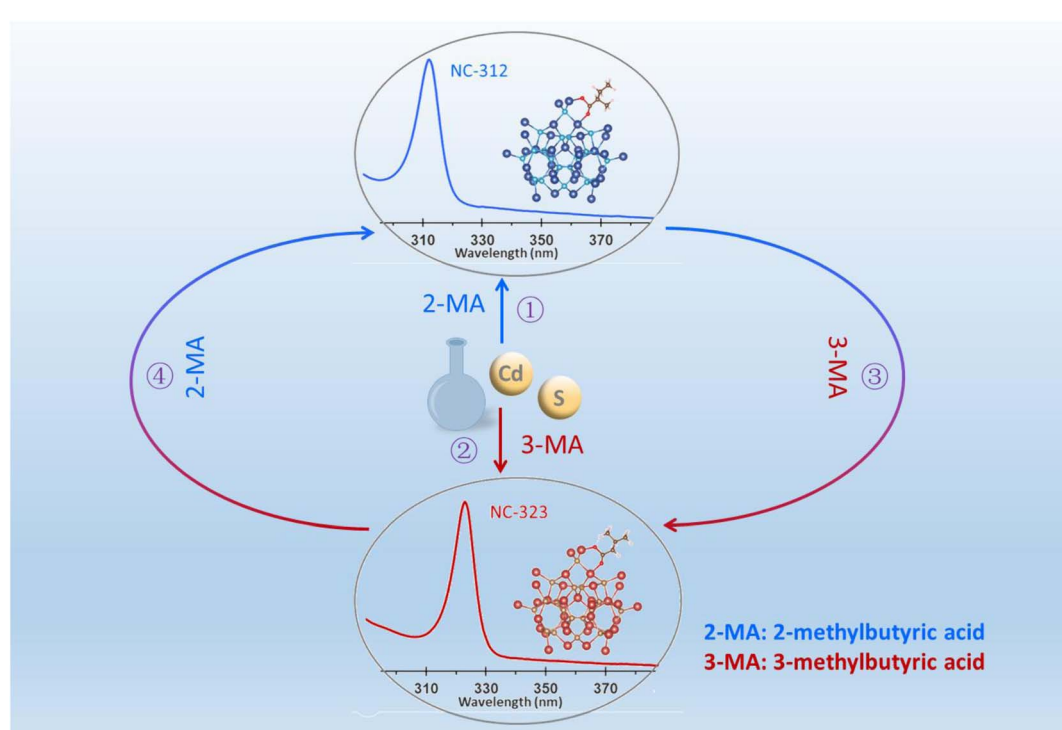
With this in mind, we develop a novel strategy for the selective synthesis of CdS NC isomers by judiciously choosing a pair of isomeric carboxylic acids, 2-methylbutyric acid and 3-methylbutyric acid (hereafter abbreviated as 2-MA and 3-MA). As illustrated in Scheme 1, CdS NC-312 and NC-323 (denoted by their absorption peak position) were selectively generated with the presence of 2-MA (①) and 3-MA (②), respectively. Alternatively, the as-synthesized NC-312 (③) and NC-323 (④) were interconvertible by re-adding this pair of carboxylic acid isomers. Together with density functional theory (DFT) calculations of CdS NC isomer models, we provide a comprehensive insight into the carboxylic acid isomer induced selective synthesis of NC isomers.

Results and discussion

Synthesis and characterization of CdS nanocluster isomers

In a typical synthesis, a pair of isomeric carboxylic acids (2-MA and 3-MA) were added to a precursor mixture, consisting of cadmium oleate (Cd(OA)_2) and S powder in 1-octadecene (ODE). With the addition of 2-MA and 3-MA, CdS NC-312 and NC-323 were formed, respectively (see ESI for details†). This pair of isomeric carboxylic acids share the same formula but different structures by changing a methyl side group from α to β position (Fig. 1a). As shown in Fig. 1b, the synthesized two isomeric CdS

NCs exhibited narrow absorption peaks at 312 and 323 nm, with a full-width at half-maximum (FWHM) of ~ 10 nm. The transmission electron microscopy (TEM) images of purified NC-312 and NC-323 show dot-like morphology with an approximate diameter of 3 nm (Fig. 1c). Considering the resolution of our TEM images and slight aggregation of NCs, we may not extract the accurate size of NCs.^{30,31} The corresponding absorption spectra of as-synthesized and purified NCs are shown in Fig. S1,† indicating that no transformation occurred during the purification process. Compositional and structural characterization were performed for the obtained isomeric NCs. Matrix-assisted laser desorption/ionization time-of-flight (MALDI-TOF) mass spectrometry (MS) was employed to explore the mass of the two CdS isomers. Both NC-312 and NC-323 exhibited a peak at around $m/z = 5187$ Da in their mass spectra, similar to what has been observed for $\text{Cd}_{34}\text{S}_{33}$ (oleic acid) clusters,³² indicating that the two NCs have similar mass (Fig. 1d). The thermogravimetric analysis (TGA) demonstrates that NC-312 and NC-323 have similar weight ratios of inorganic cores to organic ligands (Fig. S2†), indicating that the two isomers have the same CdS inorganic core composition. The X-ray diffraction (XRD) patterns of the isomers are presented in Fig. 1e. The broad diffraction peaks shown in the XRD pattern were attributed to the small size of isomers.³³ In addition, a shoulder at $2\theta \sim 37^\circ$ is observed in the XRD pattern of NC-323 but not in that of NC-312, suggesting their respective wurtzite-like and zinc blende-like structures.^{16,34} The Cd 3d X-ray photoelectron spectra (XPS) of NC-312 and NC-323 are shown in Fig. 1f. The two isomeric NCs exhibited similar characteristic peaks that are assigned to $\text{Cd 3d}_{5/2}$ and $\text{Cd 3d}_{3/2}$. A slight peak



Scheme 1 Illustration of the isomeric carboxylic acids induced the selective synthesis of CdS nanocluster isomers NC-312 and NC-323 (① and ②) and their interconversion (③ and ④).



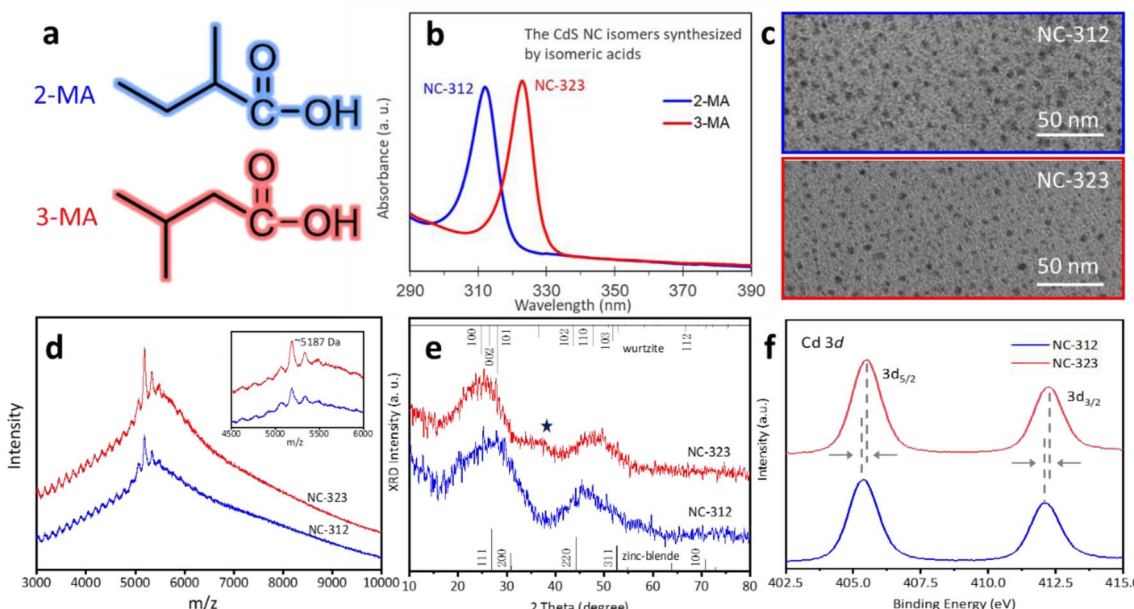


Fig. 1 (a) The molecular structure of the isomeric carboxylic acids. (b) UV-vis absorption spectra, (c) TEM images, (d) MALDI-TOF mass spectra, (e) XRD patterns, and (f) Cd 3d XPS spectra of CdS NC-312 and NC-323.

shift to higher binding energy was observed for NC-323, suggesting again the structural transformation from zinc blend to wurtzite.^{35,36} The combined results suggest that the generated NC-312 and NC-323 are isomeric NCs with similar mass but slightly different structures, similar to the previously reported CdS isomers, which are referred to as MSC-311 and MSC-322.¹⁵ Crucially, our synthesized CdS NC-312 and NC-323 exhibit a strict isomeric relationship, sharing both the isomeric inorganic core and organic surface by use of the isomeric acids. On the other hand, the employed isomeric acids not only influence the structure of NCs, but also improve their thermal stability, to further advance their optoelectronic and catalytic applications. The thermal stability of our synthesized NCs was compared with that of the reported CdS MSCs with capping of oleic acid (OA).¹⁵ As shown in Fig. S3,† OA capped CdS MSCs decomposed rapidly within 1 min followed by the formation of conventional quantum dots (QDs) when aged at 180 °C. However, our synthesized NC-312 and NC-323 grew consistently at 180 °C for 1 hour without QD nucleation. This observation suggests that the thermal stability of our NCs capped with isomeric ligands was obviously enhanced compared to that of the OA capped MSCs. The improved stability of NC isomers may be attributed to the stronger coordination ability to Cd of the employed isomeric acids than that of OA.

Isomerization between NC-312 and NC-323

Compared with the QDs, the NCs are more sensitive to their surface environment, making ligand exchange effective for inducing structural changes. Therefore, we further studied the isomerization between NC-312 and NC-323 through using the as-synthesized NC-312 and NC-323 as starting materials. In a typical ligand-exchange reaction, 2 mL of 2-MA capped NC-

312 and 3-MA capped NC-323 were mixed with the same amount of 3-MA and 2-MA at 25 °C in air, respectively. Aliquots were taken from the mixture by time and dispersed in hexane for absorption measurement. The evolution of the ligand-induced isomerization between NC-312 and NC-323 was monitored by UV-vis spectroscopy (Fig. 2). In the presence of 3-MA (76 µL), the intensity of NC-312 decreased as NC-323 formed gradually. After 56 hours, most of the NC-312 disappeared while a significant amount of NC-323 formed without the co-production of other NC species or QDs during the transformation. The isosbestic point at 317 nm was observed during the transformation process, indicating that the transformation from NC-312 to NC-323 is direct one-to-one interconversion without any intermediates involved (Fig. 2a). Similar to this, by adding 76 µL of 2-MA, 3-MA capped NC-323 was successfully converted to NC-312 in 360 hours with an obvious conversion hysteresis before the reaction time of 144 hours¹⁶ (Fig. 2b). Obviously, the 2-MA induced NC-323 to NC-312 isomerization was significantly slower than NC-312 \Rightarrow NC-323 isomerization. Control experiments were carried out by aging NC-312 and NC-323 in air without adding isomeric acids (Fig. S4†). No conversion occurs, and both NCs were stable during the aging. Note that the isomerization from NC-323 to NC-312 was also successfully performed in a glovebox (Fig. S5†). Combined with the blank experiment (Fig. S4†), we believe that ligand exchange is the dominant driving force for the isomerization in this study. The effect of varied amounts of added acids on the isomerization can be found in Fig. S6.† Furthermore, we performed a kinetic study for the isomerization between NC-312 and NC-323 by the raw variation of the optical density of the reactant. The evolution of the absorbance of the reactant fits well with the first-order reaction equation described by (1):



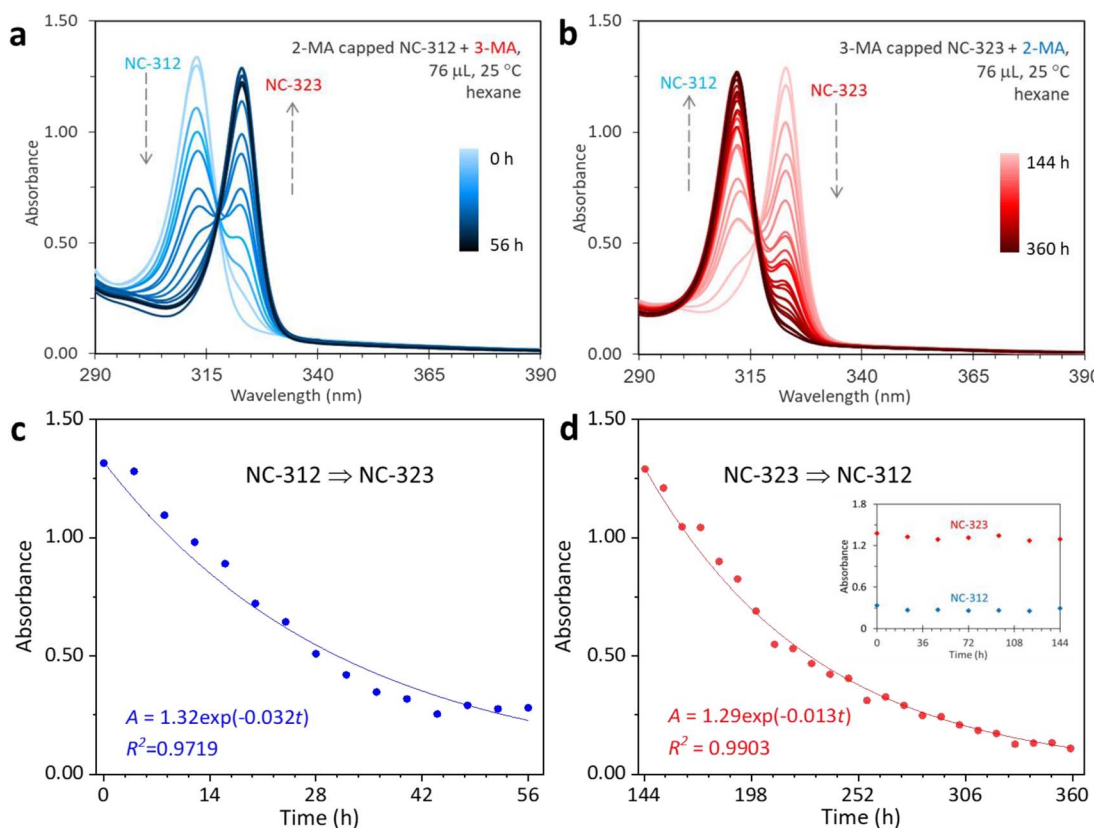


Fig. 2 (a) NC-312 conversion to NC-323 with the presence of 3-MA at 25 °C in air. Aliquots (25 μ L) were extracted from the mixture of NC-312 (2 mL) and 3-MA (76 μ L) for up to 56 hours with an interval of 4 hours, and dispersed in 3.0 mL of hexane for UV-vis absorption spectra collection. (b) NC-323 transformation to NC-312 with the addition of 2-MA at 25 °C. There were 24 spectra collected from 144 to 360 hours with time intervals of 8 hours. Of note, NC-323 to NC-312 transformation exhibits an obvious conversion hysteresis before the reaction time of 144 hours (inset of Fig. 2d). Kinetics study of the NC-312 \Rightarrow NC-323 (c) and NC-323 \Rightarrow NC-312 isomerization (d). The time-dependent absorbance (A) of the reactants (solid dots) was fitted by the first-order reaction equations (solid trace).

$$A = A^0 \exp(-kt) \quad (1)$$

where k is the rate constant. A is the time-dependent absorbance of the reactants, A^0 is the initial absorbance of the reactants. The kinetic study reveals that $\text{NC-312} \Rightarrow \text{NC-323}$ and $\text{NC-323} \Rightarrow \text{NC-312}$ isomerization followed closely first-order reaction kinetics with a rate constant of 0.032 hours⁻¹ and 0.013 hours⁻¹, respectively. The Arrhenius plots suggest that the activation energy (E_a) values for the isomerization from NC-312 to NC-323 and from NC-323 to NC-312 were 179.7 and 47.9 kJ mol⁻¹, respectively (Fig. S7†). The activation energies in our study are lower than previously reported energies for a similar reversible transformation of CdS MSCs.¹⁵ We speculate that the added acids here not only serve as the ligands of NCs but also play a role of a “catalyst”, similar to the use of methanol for accelerating the evolution from an immediate precursor to CdS MSC-311.³⁷

The slower conversion rate of NC-323 to NC-312 suggests that 3-MA has stronger coordination capacity to Cd than 2-MA. To further investigate the binding capacity of 2-MA and 3-MA, we performed three reactions of $\text{Cd(OA)}_2 + \text{SODE}$ by adding a 2-MA and 3-MA mixture with a total volume of 190 μ L. Fig. S8† presents the temporal evolution of UV absorption spectra of samples extracted from the three reactions. NC-312 was predominately

formed during the whole reaction when the volume ratio of 2-MA to 3-MA was 3 : 1. As the amount of 3-MA increased, NC-312 produced at the initial stage and finally transformed to NC-323. In particular, NC-323 eventually formed when the volume ratio of 2-MA to 3-MA was 1 : 1. Therefore, it is reasonable to conclude that 3-MA has stronger coordination ability to Cd than that of 2-MA, which is consistent with the slight shifting towards higher binding energy of $\text{Cd} 3d_{5/2}$ and $\text{Cd} 3d_{3/2}$ peaks for NC-323 in the XPS spectra.³⁸ To support our hypothesis, DFT calculation of the Gibbs free energy ΔG was performed for $\text{Cd}(2\text{-MA})_2$ and $\text{Cd}(3\text{-MA})_2$ molecules (Fig. S9†). The ΔG of $\text{Cd}(2\text{-MA})_2$ and $\text{Cd}(3\text{-MA})_2$ were -166.28 kJ mol⁻¹ and -168.53 kJ mol⁻¹, respectively. The lower ΔG of $\text{Cd}(3\text{-MA})_2$ than that of $\text{Cd}(2\text{-MA})_2$ suggests that 3-MA has stronger coordination ability to Cd than 2-MA, resulting in the higher stability of $\text{Cd}(3\text{-MA})_2$.

DFT calculations of CdS clusters coordinated with isomeric acids

The absorption spectra of NCs are crucially dependent on their structures.³⁹ To identify the determination effect of isomeric acids on the structure of NCs, we performed a simulation on the absorption spectra of pristine CdS clusters capped with 2-MA or 3-MA.⁴⁰ The structural model of the pristine CdS cluster was

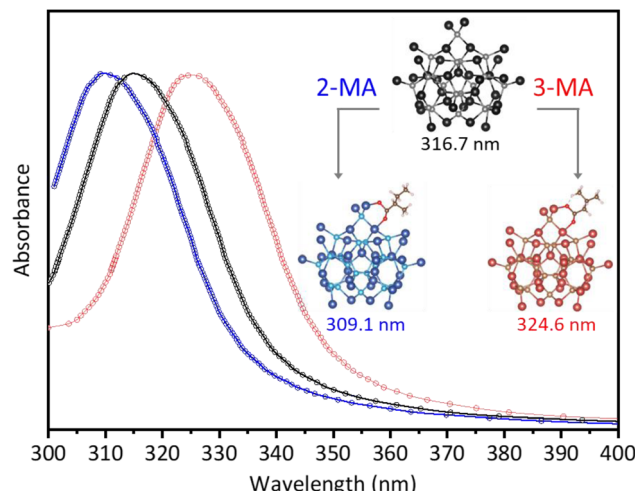


Fig. 3 The computed absorption spectra of pristine $\text{Cd}_{37}\text{S}_{20}$ clusters (black trace) with a 2-MA (blue trace) or 3-MA (red trace) molecule coordinated. The corresponding structural models are shown in the inset.

suggested as the well-established $\text{In}_{37}\text{P}_{20}$ cluster by substituting In and P atoms with Cd and S.^{16,39} As shown in Fig. 3, the calculated absorption spectra of the pristine CdS cluster exhibited a single peak at 316.7 nm (black trace). When

coordinated with a 2-MA molecule, the absorption peak of the CdS cluster blue-shifted to 309.1 nm (blue trace), aligned with the characteristic absorption of the synthesized NC-312 in the presence of 2-MA. Correspondingly, the absorption peak of the CdS cluster red-shifted to 324.6 nm (red trace) when 3-MA capped, similar to the characteristic absorption of NC-323. The corresponding structures of the isomeric NCs are shown in the inset of Fig. 3. The calculated energy for NC-312 (-326.13 eV) was higher than that for NC-323 (-326.83 eV), suggesting superior stability for NC-323 than NC-312. Furthermore, the calculated adsorption energies of NC-312 and NC-323 were -1.94 and -2.28 eV, respectively. This trend was also evident when the structural models of the isomeric NCs were built by pristine CdS clusters with two 2-MA or 3-MA coordinated (Fig. S10†). Overall, the modeling is consistent with our experimental observations that 2-MA and 3-MA have specific selectivity for the formation of CdS NC isomers. Note that a hydrogen bond formed between the 3-methyl group and the carboxylate group of 3-MA enables the formation of a six-member ring structure when 3-MA coordinated to the surface of NC-323 (Fig. S10†). We speculate that the formation of the six-member ring might lead the rearrangement of the Cd and S atoms on the surface of the clusters and induce the overall isomerization. The Fourier transform infrared (FTIR) spectroscopic study of the isomerization shows that the difference between the carboxylate asymmetric stretches (ν_{as}) and

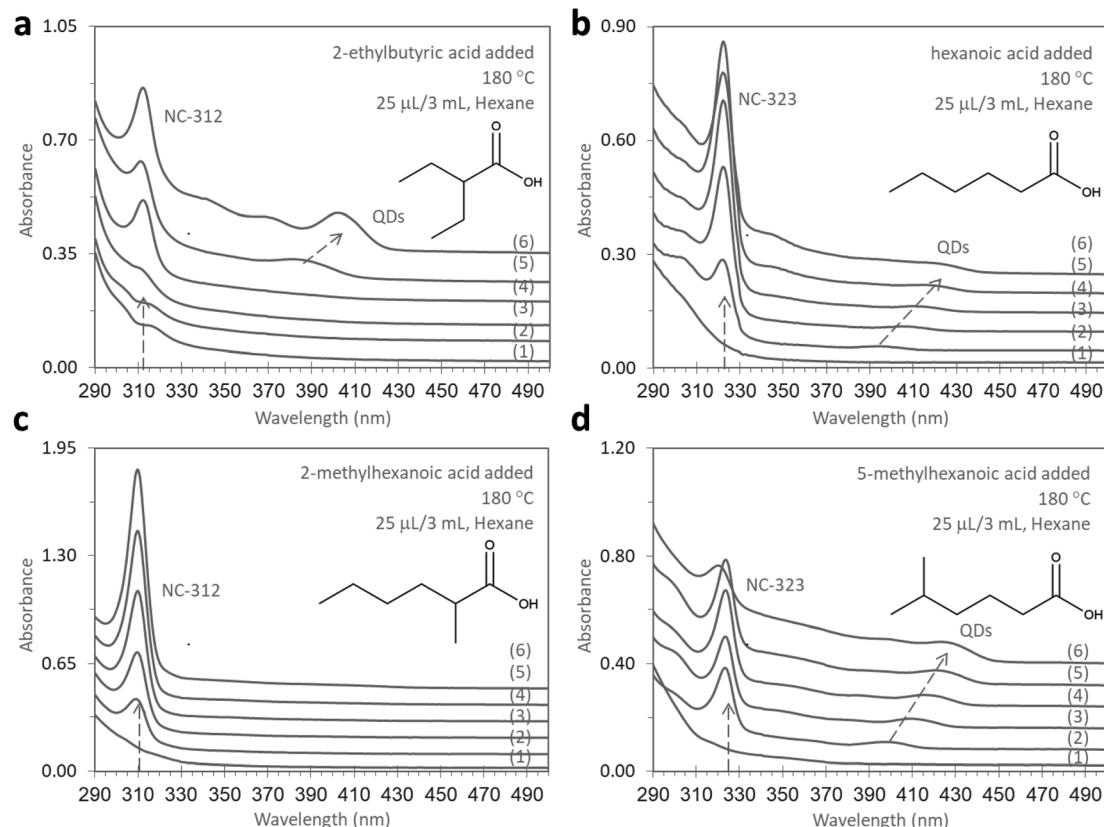


Fig. 4 Absorption spectral evolution of samples extracted from 4 batches. Isomeric 2-ethyl butyric acid (a) and hexanoic acid (b), 2-methylhexanoic acid (c) and 5-methylhexanoic acid (d) were added. Six samples were extracted at $180\text{ }^{\circ}\text{C}$ with reaction times of (1) 10 min, (2) 15 min, (3) 25 min, (4) 40 min, (5) 70 min, and (6) 130 min. The inset shows the molecular structure of the isomeric carboxylic acids.

symmetric stretches (ν_s) had no obvious change (Fig. S11†). Therefore, we speculate that the surface reconfiguration is initiated by the steric pressure changes in the ligand sphere,⁴¹ which is different from the changes in ligand-binding modes induced the surface reconfiguration.¹⁶ The intriguing aspect lies in how the nuanced variations in the additive structure can give rise to profound effects on the overall configuration of NCs. Further investigation is required to explore the molecular-level mechanism of NC isomerization induced by the isomeric carboxylic acids.

Selective synthesis of CdS NC isomers by additional isomeric acid pairs

The generality of this simple and efficient methodology was also addressed. Two additional pairs of isomeric carboxylic acids, each comprising six and seven carbon counts, were also investigated in this study. As shown in Fig. 4, 2-ethylbutyric acid (Fig. 4a) triggered the generation of NC-312 with the co-production of QDs, while *n*-hexanoic acid (Fig. 4b) produced NC-323 as a dominant product accompanied by the formation of QDs. Similar to this, the isomeric 2-methylhexanoic acid (Fig. 4c) and 5-methylhexanoic acid (Fig. 4d) promoted NC-312 and NC-323 formation, respectively. Applying this method to other semiconductor NCs or even metallic NCs is ongoing.

Conclusions

Different structural nanocluster isomers exhibit distinct properties, making them promising candidates for diverse applications. Therefore, it is of great significance to develop simple and straightforward synthetic methods for NC isomers with desired structure. Here, we report an efficient method for selective synthesis of semiconductor nanocluster isomers, CdS NC-312 and NC-323 by introducing a pair of isomeric carboxylic acids as additives. As a result, the synthesized NC isomers demonstrated a strict isomeric relationship that involved an isomeric inorganic core and organic surface. The synthesized CdS NCs were interconvertible by re-adding the isomeric carboxylic acids. The DFT simulations further support that 2-MA and 3-MA have specific selectivity for the formation of CdS NC isomers. Specifically, a six-member ring was formed when 3-MA coordinated on the surface of the clusters, inducing the rearrangement of the Cd and S atoms on the cluster surface and resulting in the overall isomerization. This study demonstrates that the isomeric additives have obvious and efficient influence on the structure of NC products. Further work will focus on extending the isomeric additive scope, such as isomeric amines, alcohols, and thiols. We also expect that this approach can be possibly applied to a broader range, *i.e.* functional chiral materials, to advance their scientific and industrial applications further.

Data availability

All the data supporting this article have been included in the main text and the ESI.†

Author contributions

J. Z. conceived the idea and designed this work. Y. L., Z. W. and M. Z. carried out the synthesis and isomerization experiments. Q. T. contributed to the DFT calculations. J. Z. and M. L. prepared the manuscript. All authors contributed to data analysis and commented on the manuscript.

Conflicts of interest

There are no conflicts to declare.

Acknowledgements

This work has been partially supported by the Teacher Development Research Start-up Fund of Chengdu University of Technology (10912-KYQD2021-09184) and Medical-Engineering Interdisciplinary Research Foundation of Shenzhen University (2023YG012). We thank Mr Yongcheng Zhu of Huazhong University of Science and Technology for the discussion on the DFT calculations. We thank the Instrumental Analysis Center of Shenzhen University for the sample characterization.

Notes and references

- 1 A. T. Balaban, Enumeration of Isomers, *Chemical Graph Theory. Introduction and Fundamentals*, Abacus Press, 1991.
- 2 C. Dugave and L. Demange, *Chem. Rev.*, 2003, **103**, 2475–2532.
- 3 J. J. Chen, J. H. Fang, X. Y. Du, J. Y. Zhang, J. Q. Bian, F. L. Wang, C. Luan, W. L. Liu, J. R. Liu, X. Y. Dong, Z. L. Li, Q. S. Gu, Z. Dong and X. Y. Liu, *Nature*, 2023, **618**, 294–300.
- 4 J. Dai, Z. Wang, Y. Deng, L. Zhu, F. Peng, Y. Lan and Z. Shao, *Nat. Commun.*, 2019, **10**, 5182.
- 5 J. M. Hawkins and T. J. Watson, *Angew. Chem., Int. Ed.*, 2004, **43**, 3224–3228.
- 6 S. Tian, Y. Z. Li, M. B. Li, J. Yuan, J. Yang, Z. Wu and R. Jin, *Nat. Commun.*, 2015, **6**, 8667.
- 7 X. Kang and M. Zhu, *Chem. Mater.*, 2020, **33**, 39–62.
- 8 H. Qian, W. T. Eckenhoff, Y. Zhu, T. Pintauer and R. Jin, *J. Am. Chem. Soc.*, 2010, **132**, 8280–8281.
- 9 X. Liu, W. Xu, X. Huang, E. Wang, X. Cai, Y. Zhao, J. Li, M. Xiao, C. Zhang, Y. Gao, W. Ding and Y. Zhu, *Nat. Commun.*, 2020, **11**, 3349.
- 10 C. Zeng, Y. Chen, K. Iida, K. Nobusada, K. Kirschbaum, K. Lambright and R. Jin, *J. Am. Chem. Soc.*, 2016, **138**, 3950–3953.
- 11 N. Xia, J. Yuan, L. Liao, W. Zhang, J. Li, H. Deng, J. Yang and Z. Wu, *J. Am. Chem. Soc.*, 2020, **142**, 12140–12145.
- 12 Y. Chen, C. Liu, Q. Tang, C. Zeng, T. Higaki, A. Das, D. Jiang, N. L. Rosi and R. Jin, *J. Am. Chem. Soc.*, 2016, **138**, 1482–1485.
- 13 Q. Li, Y. Tan, B. Huang, S. Yang, J. Chai, X. Wang, Y. Pei and M. Zhu, *J. Am. Chem. Soc.*, 2023, **145**, 15859–15868.
- 14 Z. Qin, J. Zhang, C. Wan, S. Liu, H. Abroshan, R. Jin and G. Li, *Nat. Commun.*, 2020, **11**, 6019.



15 B. Zhang, T. Zhu, M. Ou, N. Rowell, H. Fan, J. Han, L. Tan, M. T. Dove, Y. Ren, X. Zuo, S. Han, J. Zeng and K. Yu, *Nat. Commun.*, 2018, **9**, 2499.

16 C. B. Williamson, D. R. Nevers, A. Nelson, I. Hadar, U. Banin, T. Hanrath and R. D. Robinson, *Science*, 2019, **363**, 731–735.

17 D. R. Nevers, C. B. Williamson, T. Hanrath and R. D. Robinson, *Chem. Commun.*, 2017, **53**, 2866.

18 Y. Yang, Q. Shen, C. Zhang, N. Rowell, M. Zhang, X. Chen, C. Luan and K. Yu, *ACS Cent. Sci.*, 2023, **9**, 519–530.

19 Y. Yang, Y. Li, C. Luan, N. Rowell, S. Wang, C. Zhang, W. Huang, X. Chen and K. Yu, *Angew. Chem., Int. Ed.*, 2022, **61**, e202114551.

20 C. Luan, J. Tang, N. Rowell, M. Zhang, W. Huang, H. Fan and K. Yu, *J. Phys. Chem. Lett.*, 2019, **10**, 4345–4353.

21 L. He, C. Luan, S. Liu, M. Chen, N. Rowell, Z. Wang, Y. Li, C. Zhang, J. Lu, M. Zhang, B. Liang and K. Yu, *J. Am. Chem. Soc.*, 2022, **144**, 19060–19069.

22 D. Zhu, J. Hui, N. Rowell, Y. Liu, Q. Y. Chen, T. Steegemans, H. Fan, M. Zhang and K. Yu, *J. Phys. Chem. Lett.*, 2018, **9**, 2818–2824.

23 Q. Shen, C. Luan, N. Rowell, M. Zhang, K. Wang, M. Willis, X. Chen and K. Yu, *Inorg. Chem.*, 2021, **60**, 4243–4251.

24 X. Kang and M. Zhu, *Chem. Mater.*, 2019, **31**, 9939–9969.

25 X. Kang, L. Huang, W. Liu, L. Xiong, Y. Pei, Z. Sun, S. Wang, S. Wei and M. Zhu, *Chem. Sci.*, 2019, **10**, 8685–8693.

26 X. Kang, Y. Li, M. Zhu and R. Jin, *Chem. Soc. Rev.*, 2020, **49**, 6443–6514.

27 E. M. Vogl, H. Gröger and M. Shibusaki, *Angew. Chem., Int. Ed.*, 1999, **38**, 1570–1577.

28 Z. Shen, Y. Sang, T. Wang, J. Jiang, Y. Meng, Y. Jiang, K. Okuro, T. Aida and M. Liu, *Nat. Commun.*, 2019, **10**, 3976.

29 K. Mikami and S. Matsukawa, *Nature*, 1997, **385**, 613–615.

30 M. Zanella, A. Z. Abbasi, A. K. Schaper and W. J. Parak, *J. Phys. Chem. C*, 2010, **114**, 6205–6215.

31 J. P. Wilcoxon, J. E. Martin and P. Provencio, *J. Chem. Phys.*, 2001, **115**, 998–1008.

32 Y. Yao, R. Lynch and R. D. Robinson, *J. Chem. Phys.*, 2023, **159**, 014704.

33 S. H. Tolbert and A. P. Alivisatos, *J. Chem. Phys.*, 1995, **102**, 4642–4656.

34 D. Shim, J. Lee and J. Kang, *Chem. Mater.*, 2022, **34**, 9527–9535.

35 A. S. Karakoti, S. Sanghavi, P. Nachimuthu, P. Yang and S. Thevuthasan, *J. Phys. Chem. Lett.*, 2011, **2**, 2925–2929.

36 M. Liu, B. Wang, Y. Zheng, F. Xue, Y. Chen and L. Guo, *Catal. Sci. Technol.*, 2016, **6**, 3371–3377.

37 T. Zhu, B. Zhang, J. Zhang, J. Lu, H. Fan, N. Rowell, J. A. Ripmeester, S. Han and K. Yu, *Chem. Mater.*, 2017, **29**, 5727–5735.

38 M. Liu, Y. Wang, Y. Liu and F. Jiang, *J. Phys. Chem. C*, 2020, **124**, 4613–4625.

39 Y. Zhu, X. Wang, M. Liu, Y. Zhang, S. Zhang, G. Jiang, M. T. Dove, M. Zhang and K. Yu, *Chem. Phys. Lett.*, 2021, **779**, 138870.

40 V. V. Albert, S. A. Ivanov, S. Tretiak and S. V. Kilina, *J. Phys. Chem. C*, 2011, **115**, 15793–15800.

41 S. F. Sandeno, K. J. Schnitenbaumer, S. M. Krajewski, R. A. Beck, D. M. Ladd, K. R. Levine, D. Dayton, M. F. Toney, W. Kaminsky, X. Li and B. M. Cossairt, *J. Am. Chem. Soc.*, 2024, **146**, 3102–3113.

